Supporting Information

Improved Binding Affinity and Interesting Selectivities of Aminopyrimidine-Bearing Carbohydrate Receptors in Comparison with their Aminopyridine Analogues

Jan Lippe, Wilhelm Seichter and Monika Mazik*

Institut für Organische Chemie, Technische Universität Bergakademie Freiberg,
Leipziger Straße 29, 09596 Freiberg, Germany
monika.mazik@chemie.tu-freiberg.de

1 Plots of the chemical shifts of the receptor resonances as a function of added carbohydrate (WinEQNMR program).

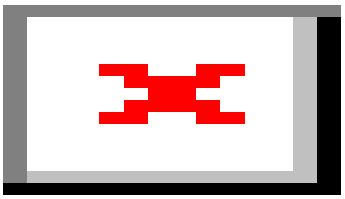	**Figure S1.** Plot of the observed chemical shifts of the NH resonances of **12** as a function of added β-galactoside **23** in $CDCl_3$ (1:1 and 1:2 receptor-sugar binding model).
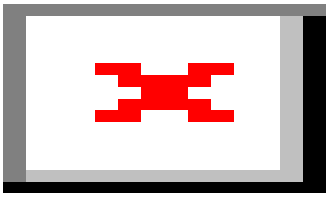	**Figure S2.** Plot of the observed chemical shifts of the pyrimidine CH resonances of **8** as a function of added β-glucoside **22** in $CDCl_3$ (1:1 and 2:1 receptor-sugar binding model).
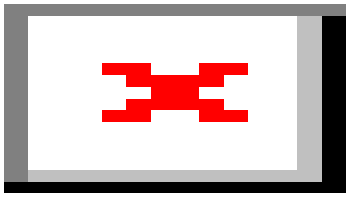	**Figure S3.** Plot of the observed chemical shifts of the Pyrimidin-CH resonances of **8** as a function of added β-galactoside **23** in $CDCl_3$ (1:1 and 2:1 receptor-sugar binding model).
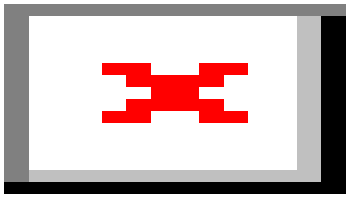	**Figure S4.** Plot of the observed chemical shifts of the pyrimidine CH resonances of **10** as a function of added β-glucoside **22** in 5/95 DMSO-d_6/$CDCl_3$ v/v (1:1 and 1:2 receptor-sugar binding model).

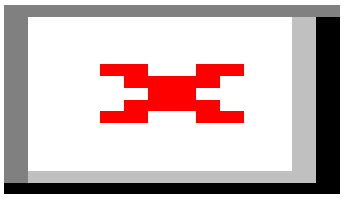	**Figure S5.** Plot of the observed chemical shifts of the pyrimidine CH resonances of **10** as a function of added β-galactoside **23** in $CDCl_3$ (1:1 and 1:2 receptor-sugar binding model).
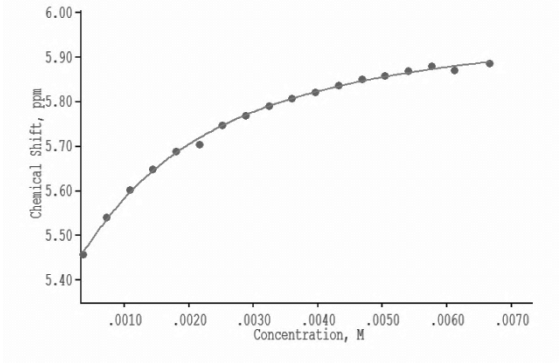	**Figure S6.** Plot of the observed chemical shifts of the NH resonances of **14** as a function of added β-galactoside **23** in $CDCl_3$(1:1 and 1:2 receptor-sugar binding model).

2 Representative HypNMR plots.

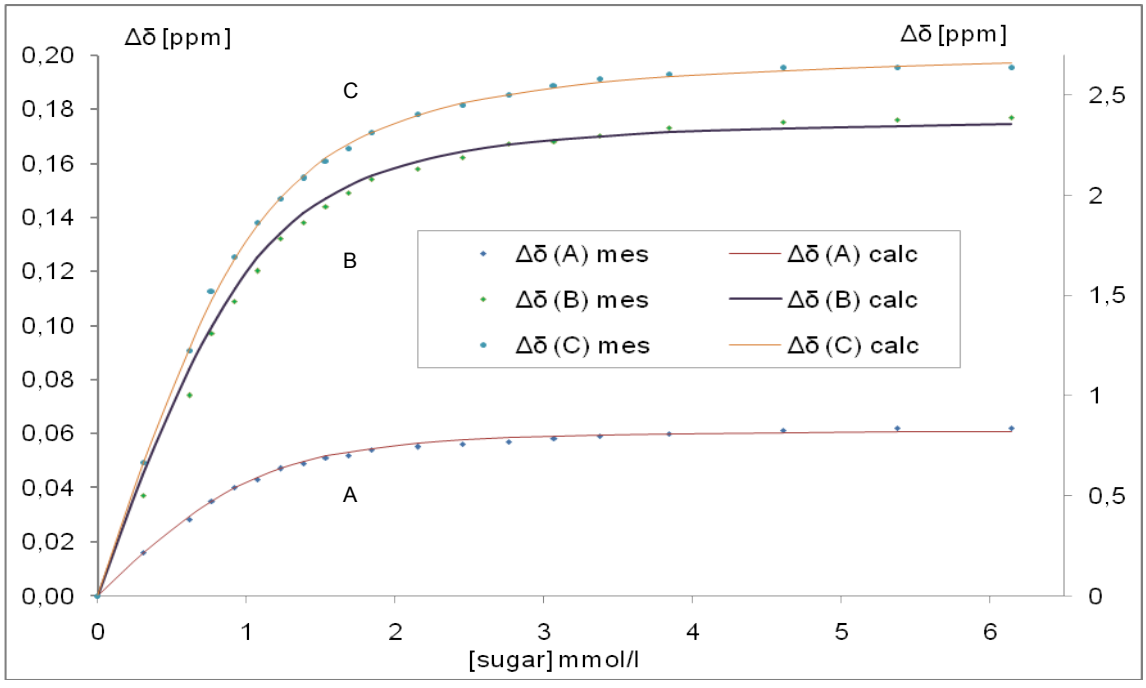

Figure S7. Plot of the calculated (line) and experimental (points) Δδ of pyrimidine C*H* (A), C*H*NH (B) and N*H* (C) signals of **8** as a function of added β-glucoside **22** in 5/95 DMSO-d_6/$CDCl_3$ (v/v). All signals are fitted simultaneously. For a better representation a secondary axis is used for C.

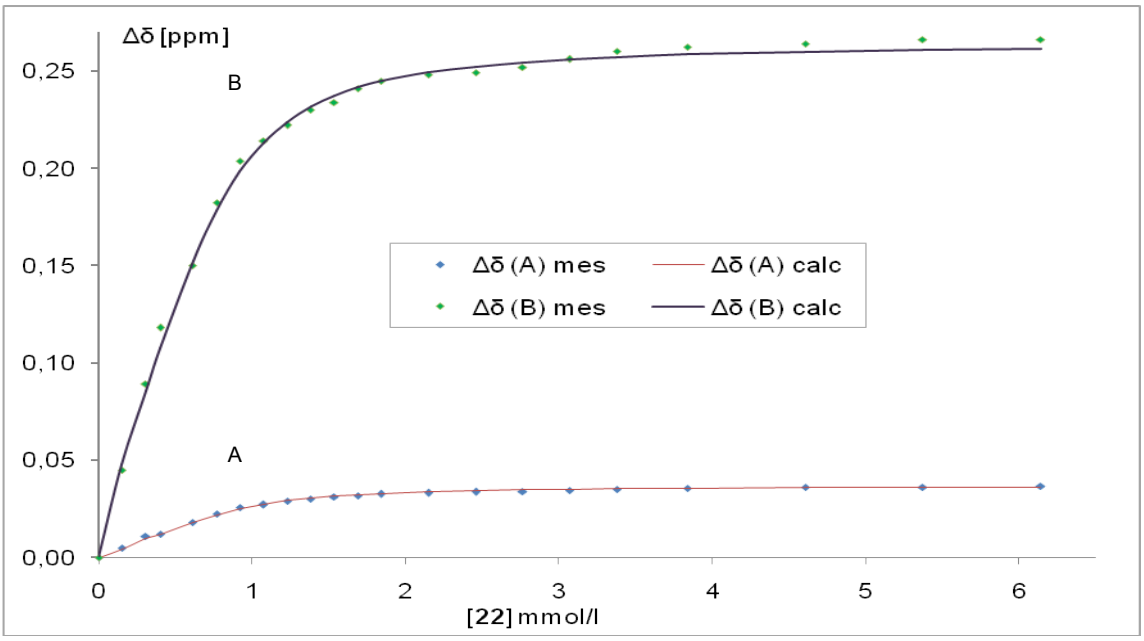

Figure S8. Plot of the calculated (line) and experimental (points) Δδ of pyrimidine C*H* (A) and C*H*NH (B) signals of **10** as a function of added β-glucoside **22** in 5/95 DMSO-d_6/$CDCl_3$ (v/v). All signals are fitted simultaneously.

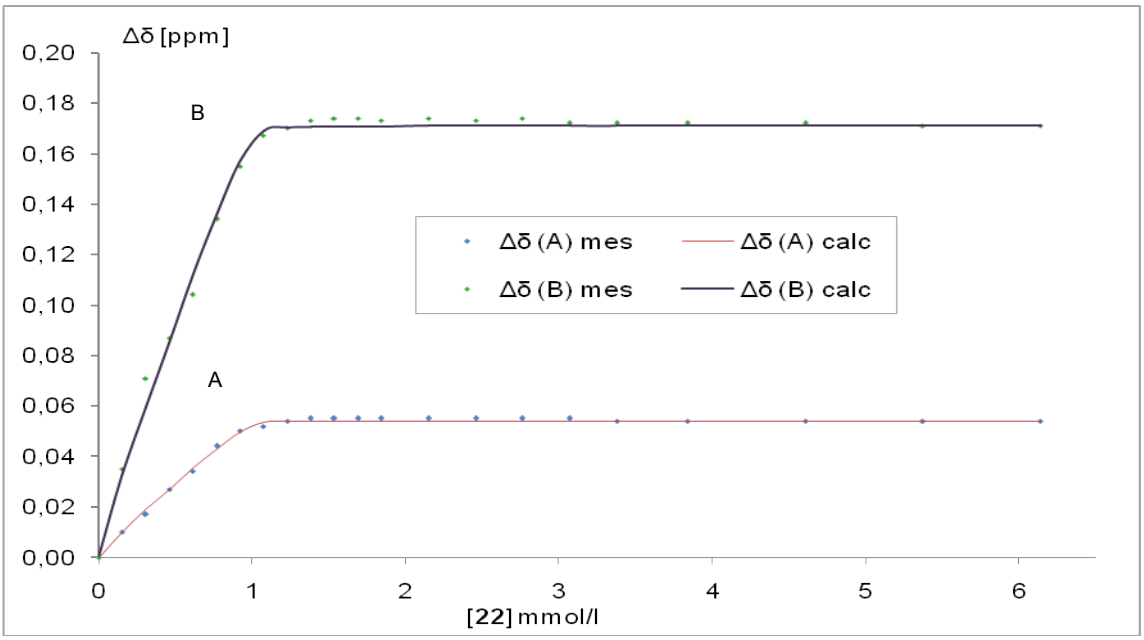

Figure S9. Plot of the calculated and experimental Δδ of pyrimidine C*H* (A) and C*H*NH (B) signals of **8** as a function of added β-glucoside **22** in $CDCl_3$; the signals are fitted simultaneously. The binding constants were too large to be accurately determined by the NMR method.

3 Representative mole ratio plots.

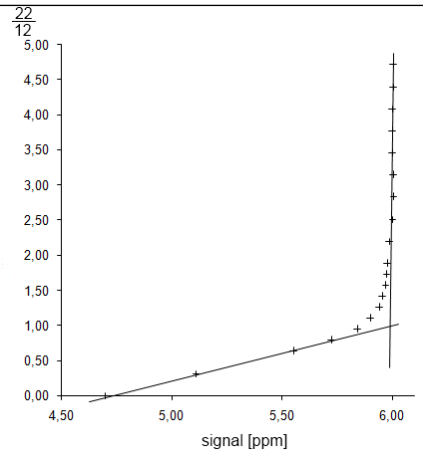

Figure S10. Mole ratio plot: Titration of compound **12** with β-glucopyranoside **22** in $CDCl_3$ (analysis of the complexation-induced shift of the NH signal of **12**).

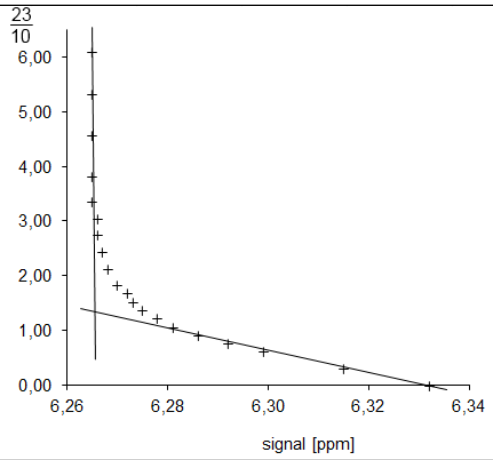

Figure S11. Mole ratio plot: Titration of compound **10** with β-galactopyranoside **23** in $CDCl_3$ (analysis of the complexation-induced shift of the pyrimidine CH signal of **10**).

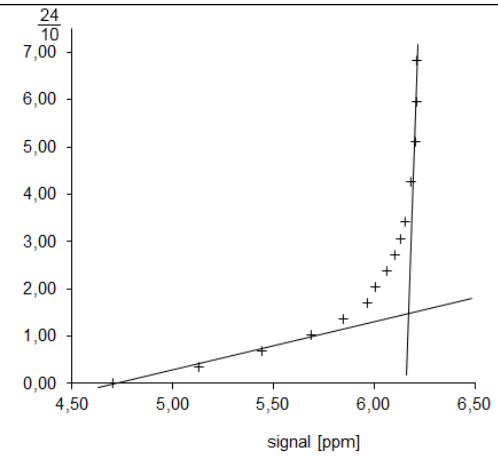

Figure S12. Mole ratio plot: Titration of compound **8** with α-glucopyranoside **24** in $CDCl_3$ (analysis of the complexation-induced shift of the NH signal of **8**).

4 ^{1}H NMR titrations of compounds **8**, **10**, **12** and **14** with the tested carbohydrates (examples).

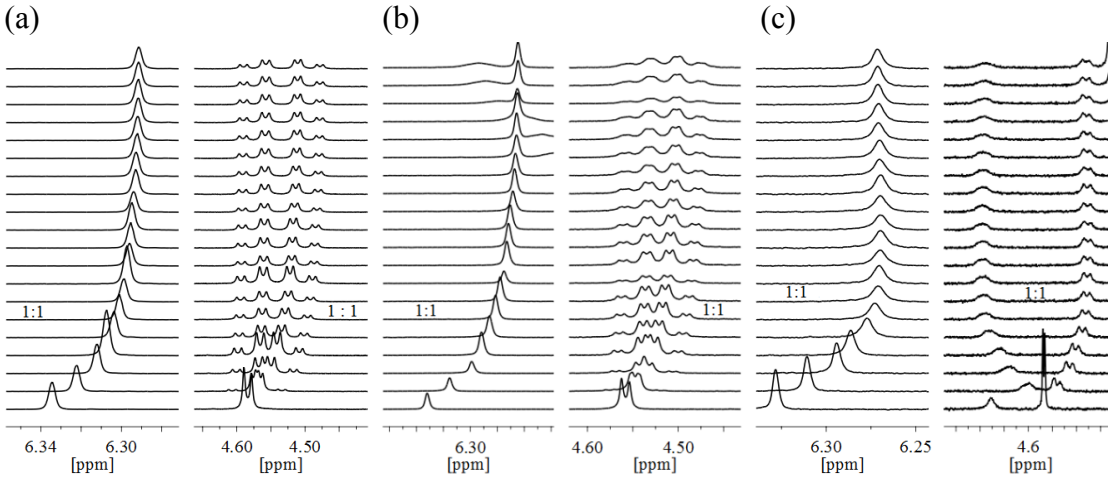

Figure S13. Partial ^{1}H NMR spectra of receptors (a) **12**, (b) **10**, and (c) **8** before (bottom) and after the addition of β-galactoside **23** in $CDCl_3$; (a) [**12**] = 1.05 mM, equiv. of **23**: 0.00-4.76; (b) [**10**] = 1.00 mM, equiv. of **23**: 0.00-6.00; (c) [**8**] = 1.02 mM, equiv. of **23**: 0.00-5.46. Shown are (from left to right) the pyrimidine CH and the CH_2 signals of the corresponding receptor.

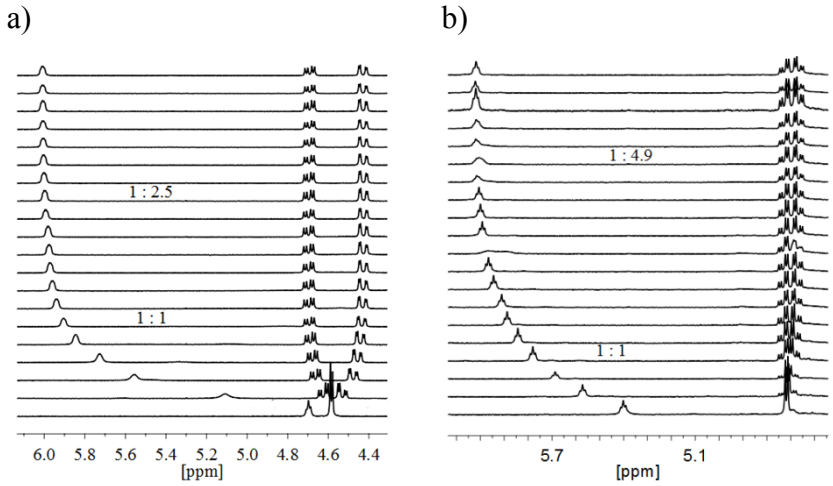

Figure S14. Partial ^{1}H NMR spectra of (a) the triethylbenzene-based receptor **12** and (b) the trimethoxybenzene-based **14** after addition of 0.00-4.70 or 0.00-5.18 equiv β-glucopyranoside **22**, respectively, in $CDCl_3$; [**12**] = 1.06 mM, [**14**] = 1.02 mM]. Shown are the NH-CH_2 signals of the corresponding receptor.

5 Molecular modelling calculations (examples).

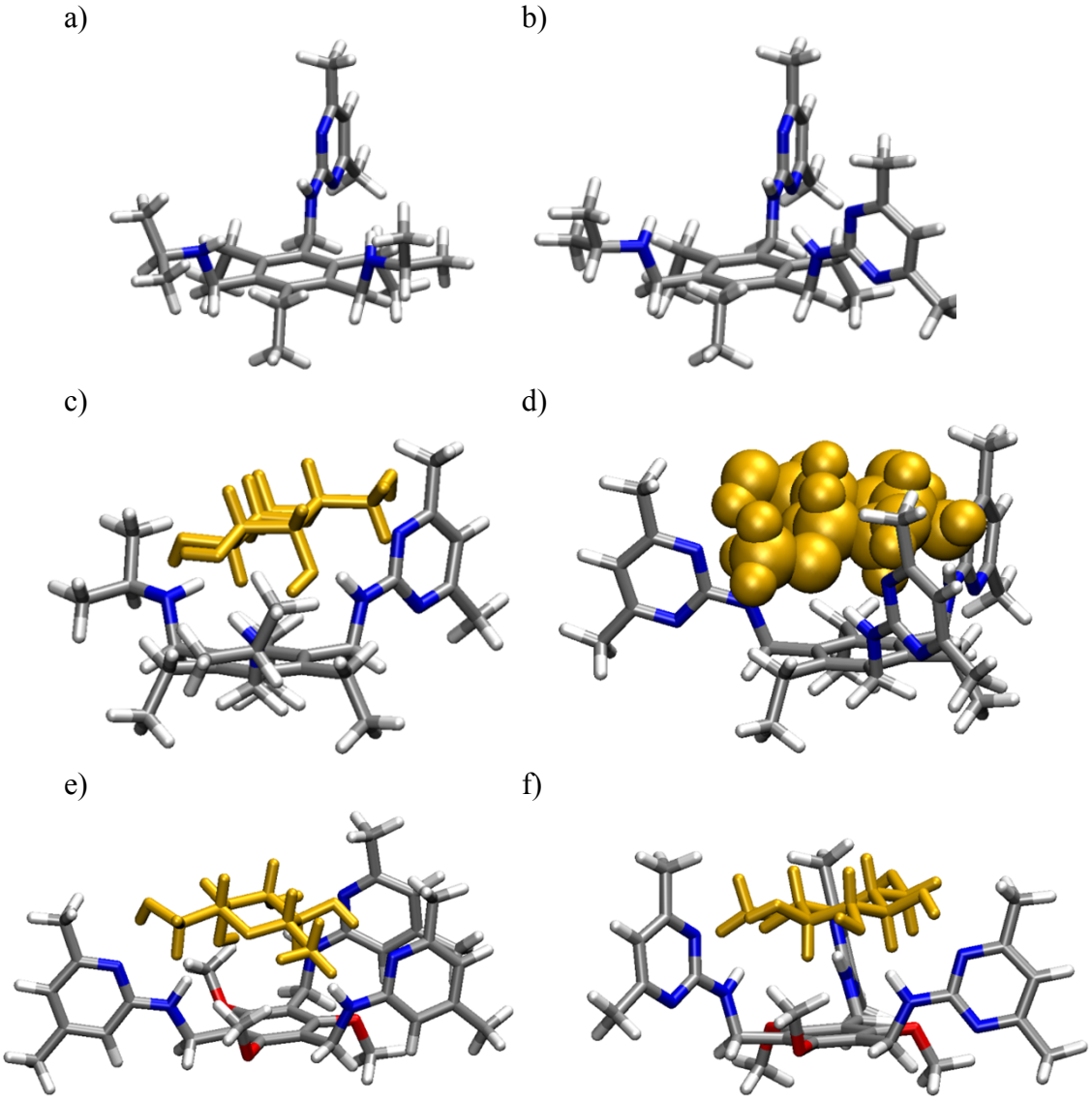

Figure S15. Energy-minimized structures of compounds (a) **8** and (b) **10** as well as of the 1:1 complexes (c) **8•24**, (d) **12•22**, (e) **13•23** and (f) **14•22.** MacroModel V.9.8, OPLS_2001 force field, MCMM, 50000 steps; . ε = 1 [F/m]. Color code: receptor N, blue; receptor C, grey; the sugar molecule is highlighted in orange.

6 Crystallographic data (Tables S1 and S2, Figure S11).

Table S1. Relevant conformational parameters of the receptor molecule in the crystal structure of **12**.

dihedral angle (°)[a]			
mpla(A)···mpla(B)	82.1(1)	mpla(A')···mpla(B')	75.0(1)
mpla(A)···mpla(C)	83.2(1)	mpla(A')···mpla(C')	82.2(1)
mpla(A)···mpla(C)	84.7(1)	mpla(A')···mpla(C')	77.0(1)
mpla(B)···mpla(C)	36.4(1)	mpla(B')···mpla(C')	39.1(1)
mpla(B)···mpla(D)	64.0(1)	mpla(B')···mpla(D')	51.9(1)
mpla(C)···mpla(D)	36.4(1)	mpla(C')···mpla(D')	87.5(1)
torsion angle (°)			
C(1)-C(13)-N(1)-C(14)	168.8(1)	C(1A)-C(13A)-N(1A)-C(14A)	170.6(1)
C(3)-C(20)-N(4)-C(21)	-127.9(1)	C(3A)-C(20A)-N(4A)-C(21A)	151.3(1)
C(5)-C(27)-N(7)-C(28)	-154.1(1)	C(5A)-C(27A)-N(7A)-C(28A)	-178.9(1)

Table S2. Distances (Å) and Angles (deg) of Non-covalent Interactions of the compound **12**.

D-H···A *Cg*···*Cg*	symmetry operator	D···A	H···A	D-H···A	
N(1)-H(1)···N(6A)	*x*, *y*, *z*	3.093(2)	2.21(1)	176(2)	Fig. S1/**a**
N(4)-H(4)···N(5A)	*x*, *y*, *z*	3.230(2)	2.40(1)	157(2)	Fig. S1/**b**
N(4A)-H(4A)···N(5)	*x*, *y*, *z*	2.992(2)	2.14(1)	162(1)	Fig. S1/**c**
N(1A)-H(1A)···C(23)[a]	*x*, *y*, *z*	3.649(3)	2.77(1)	170(2)	
N(7)-H(7)···C(23A)[a]	*x*, *y*, *z*	3.350(3)	2.49(1)	166(2)	Fig. S1/**d**
N(7A)-H(7A)···N(2A)	2-*x*, 2-*y*, -*z*	3.263(2)	2.47(1)	150(2)	
O(1W)-H(1W)···N(8)[c]	*x*, *y*, *z*	3.187(3)	2.34	179	Fig. S1/**e**
O(1W)-H(2W)···N(9A)[c]	*x*, *y*, 1+*z*	3.078(2)	2.23	133	
C(7)-H(7AA)···N(6)	*x*, *y*, *z*	3.561(2)	2.62	160	Fig. S1/**f**
C(7A)-H(7AD)···N(1A)	*x*, *y*, *z*	3.352(2)	2.62	131	Fig. S1/**g**
C(19)-H(19B)···N(6)	1+*x*, *y*, *z*	3.504(3)	2.58	158	
C(19A)-H(19F)···O(1W)	1-*x*, 2-*y*, 1-*z*	3.363(3)	2.62	133	
C(20A)-H(20C)···N(2)	*x*, *y*, *z*	3.370(2)	2.69	127	
C(16)-H(16)···*Cg*(C)[b]	1+*x*, *y*, *z*	3.633(3)	2.78	150	
C(19)-H(19C)···*Cg*(A)[b]	2-*x*, 2-*y*, 1-*z*	3.452(3)	2.60	145	
C(26)-H(26B)···N(3A)	*x*, *y*, *z*	3.551(2)	2.58	171	Fig. S1/**h**
C(11A)-H(11C)···N(7A)	*x*, *y*, *z*	3.217(2)	2.51	128	Fig. S1/**i**
C(30A)-H(30A)···*Cg*(C')[b]	2-*x*, 1-*y*, -*z*	3.758(3)	2.82	169	
Cg(A)···*Cg*(C')[b]	*x*, *y*, *z*	3.791(2)			Fig. S1/**j**

[a] In oder to obtain a reasonable hydrogen bond geometry an individual atom instead of the center of the aromatic ring was chosen as an acceptor.

[b] *Cg* means the centroid of the aromatic ring. Ring A: C(1)...C(6); ring C: N(5),N(6),C(21)...C(24); ring C': N(5A),N(6A),C(21A)...C(24A).

[c] The water hydrogen atoms were included in the model in positions which allow reasonable hydrogen bond geometries.

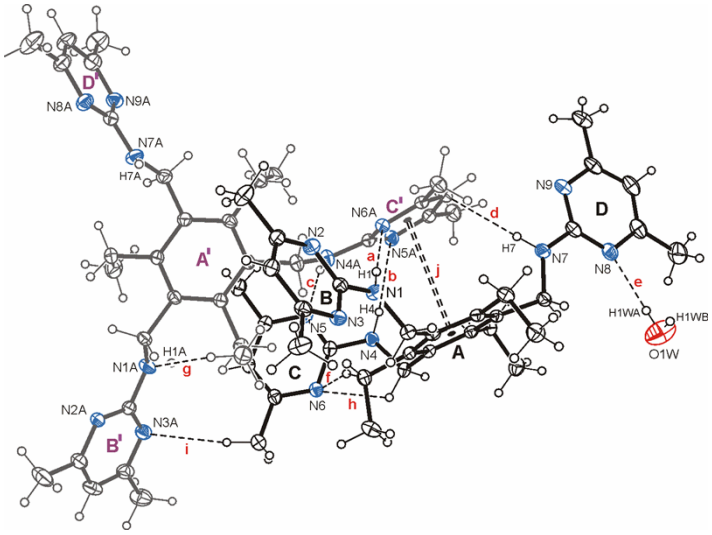

Figure S16. Perspective view of the molecular structure **1**•H_2O (2:1). The aromatic rings of one molecule are marked as A-D, whereas those of the second molecule as A´-D´; the distances and angles of the noncovalent interactions a-j are given in Table S2 The thermal ellipsoids are drawn at the 50% probability level. Nitrogen atoms are displayed as blue, the oxygen atom as red ellipsoids. Dashed lines represent hydrogen bonds, dashed double lines π···π arene stacking.

7. ^{1}H and ^{13}C NMR spectra of compounds **8-10** and **12-14** (Figures S12-27).

7.1 ^{1}H and ^{13}C NMR spectra of compound **8**.

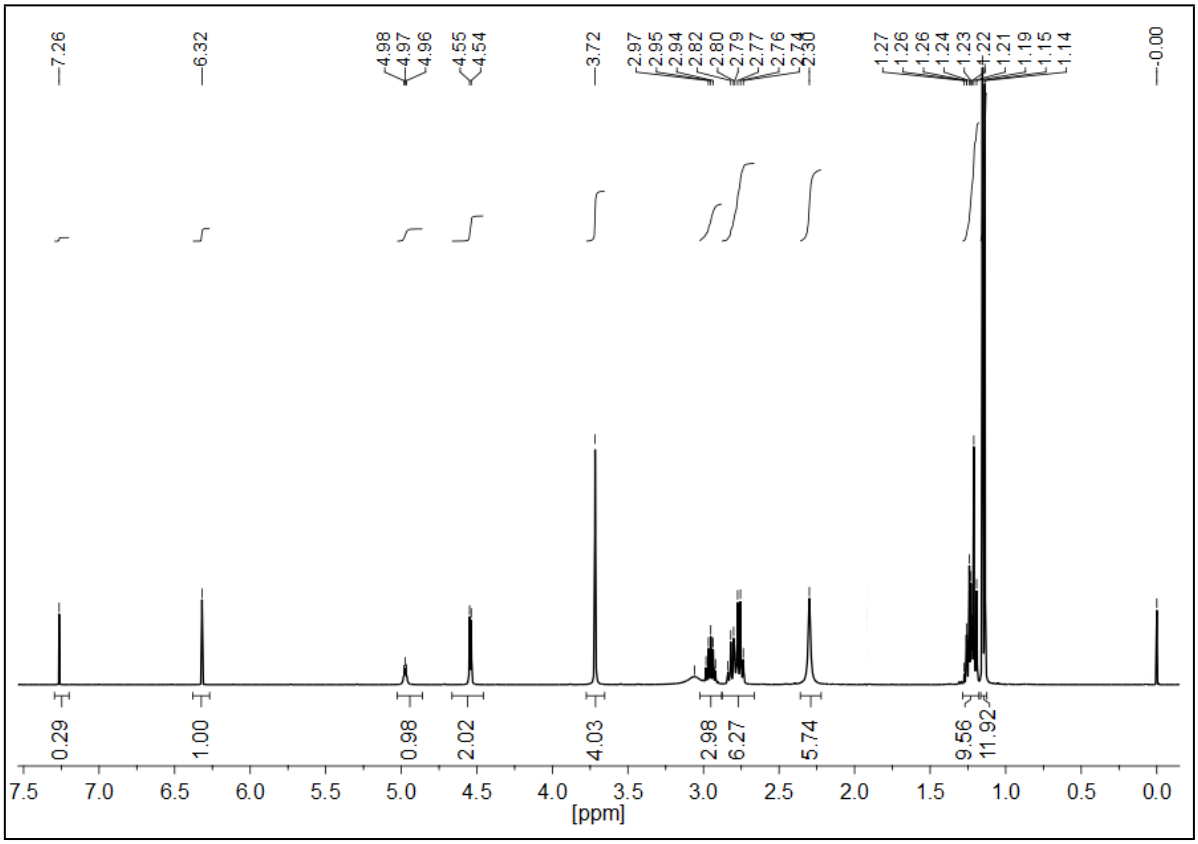

Figure S17. ^{1}H NMR spectrum of **8** in $CDCl_3$ (0.03 M).

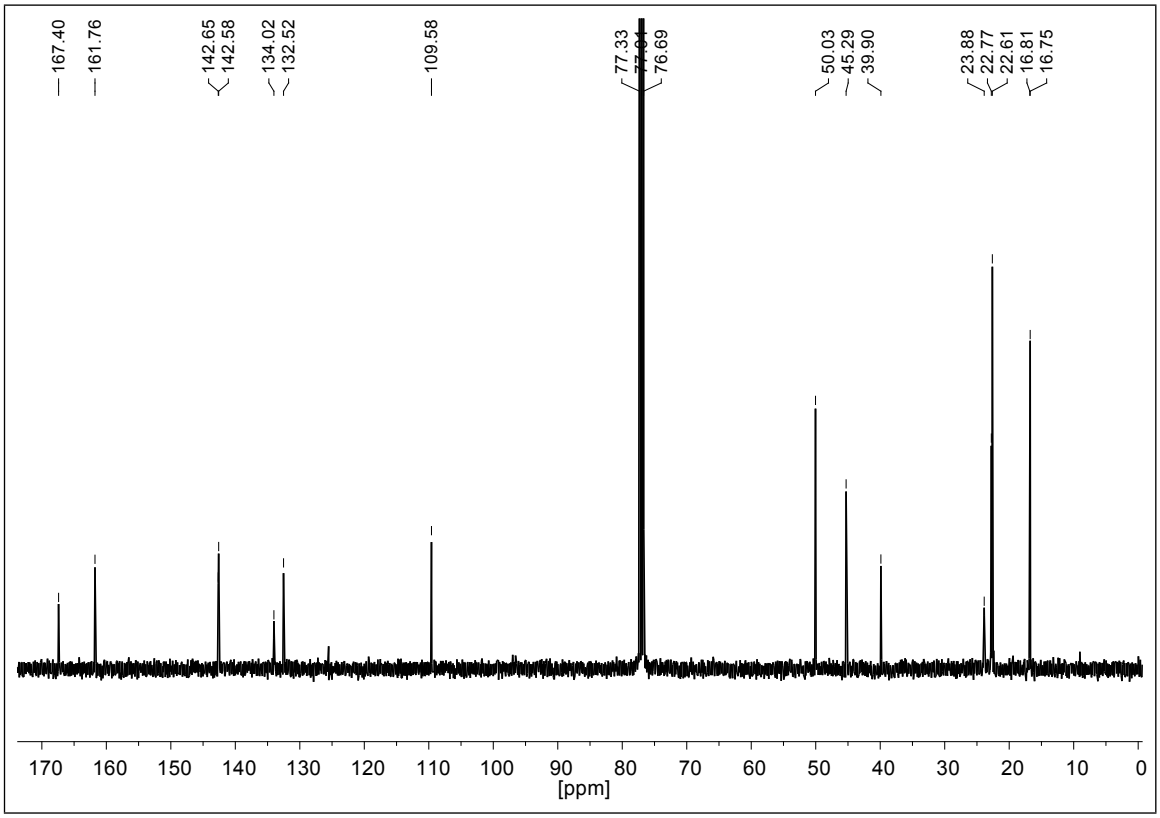

Figure S18. ^{13}C NMR spectrum of **8** in $CDCl_3$.

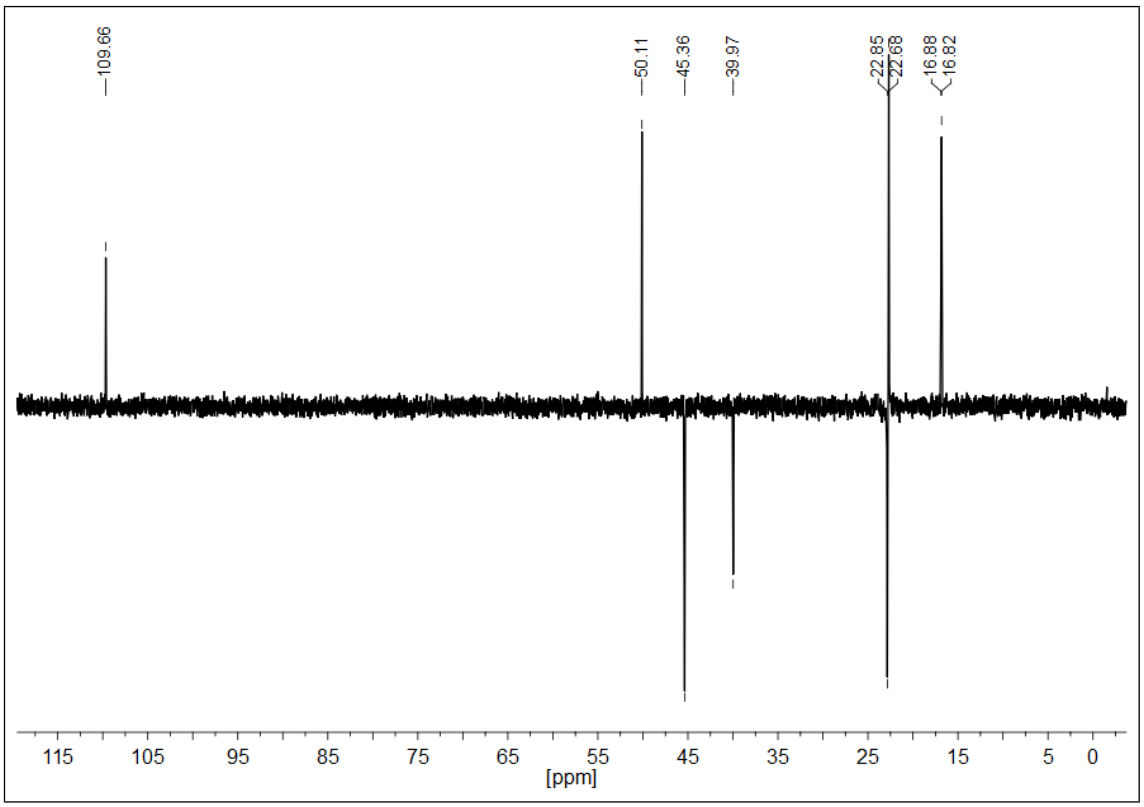

Figure S19. DEPT spectrum of **8** in $CDCl_3$.

7.2 ^{1}H and ^{13}C NMR spectra of compound **9**.

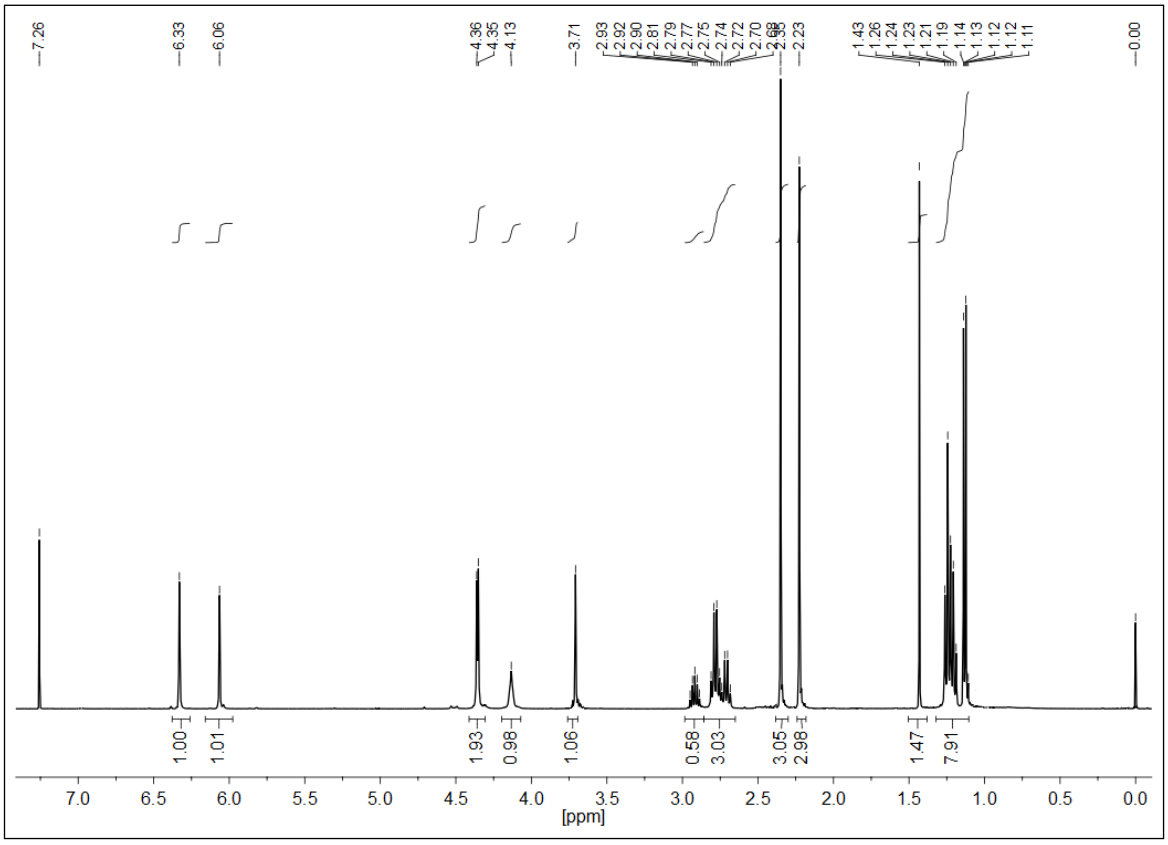

Figure S20. ^{1}H NMR spectrum of **9** in $CDCl_3$ (0.04 M).

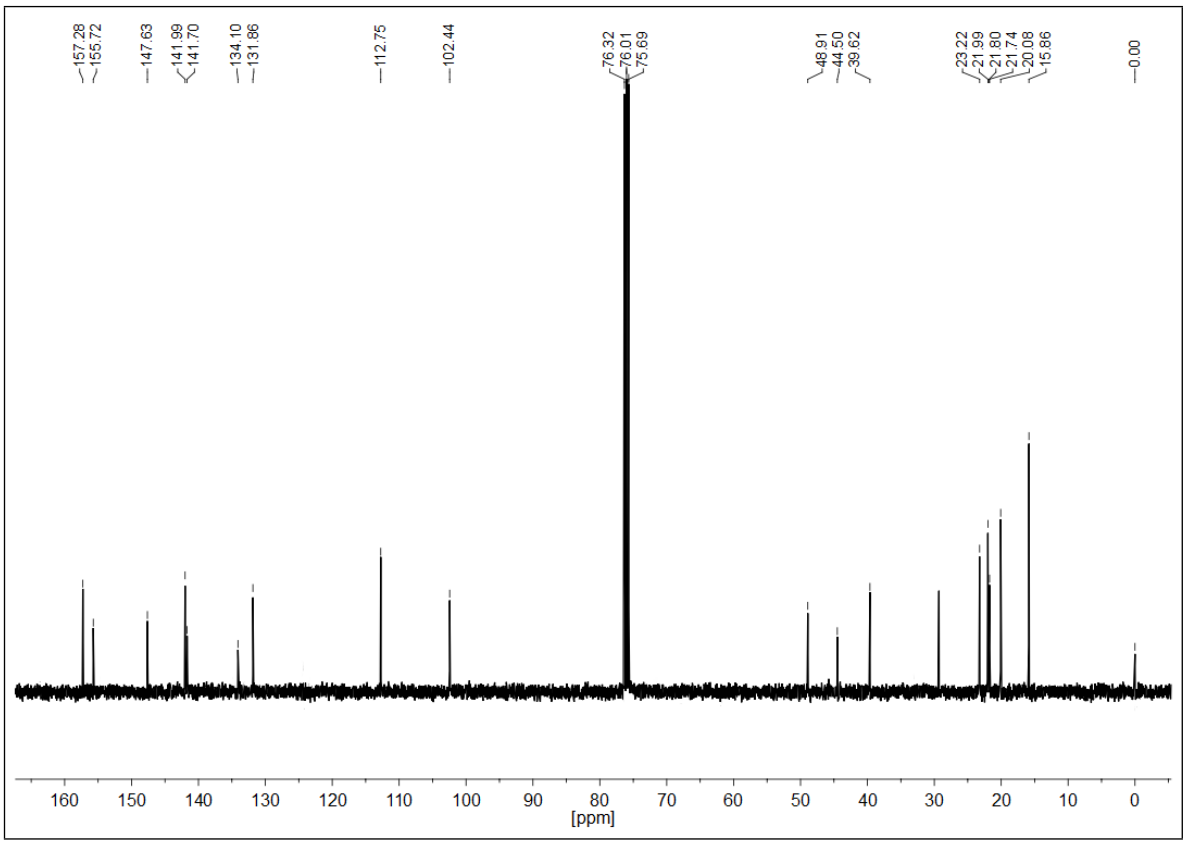

Figure S21. ^{13}C NMR spectrum of **9** in $CDCl_3$.

7.3 ^{1}H and ^{13}C NMR spectra of compound **10**.

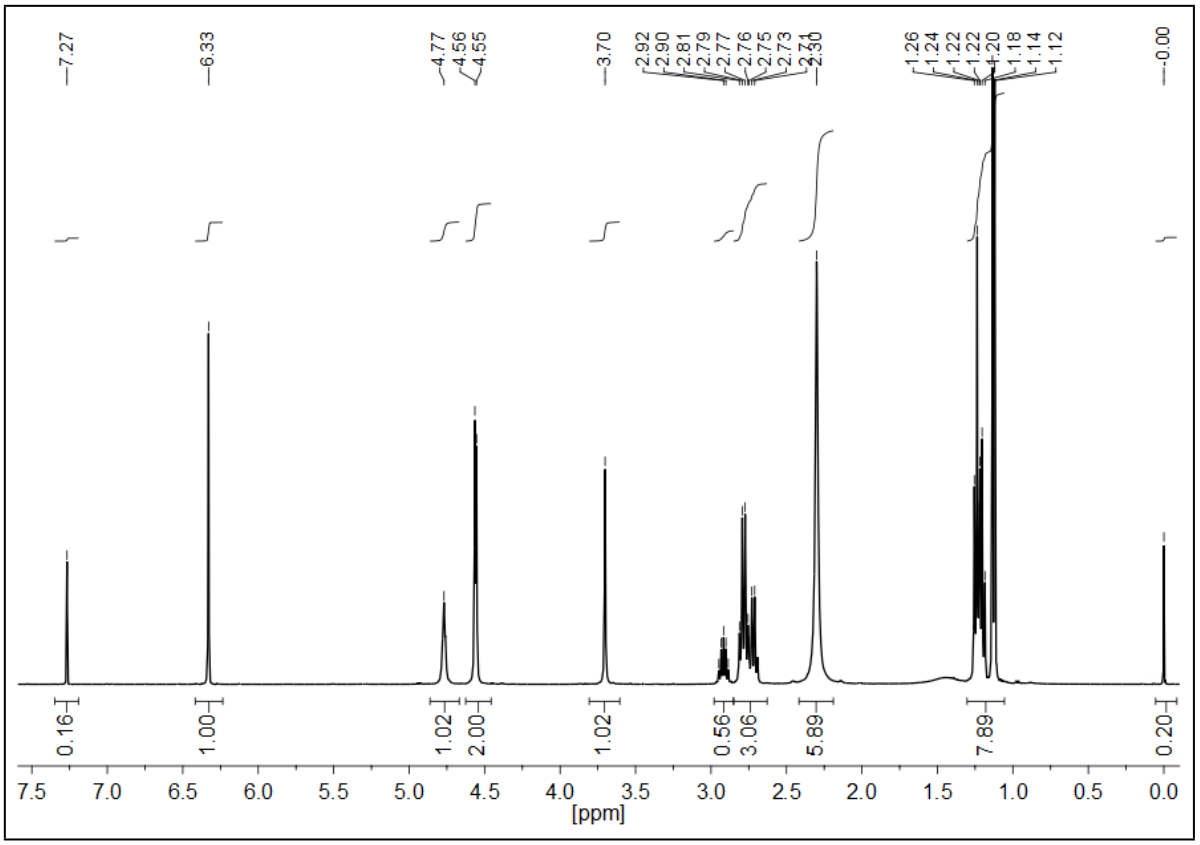

Figure S22. ^{1}H NMR spectrum of **10** in $CDCl_3$ (0.03 M).

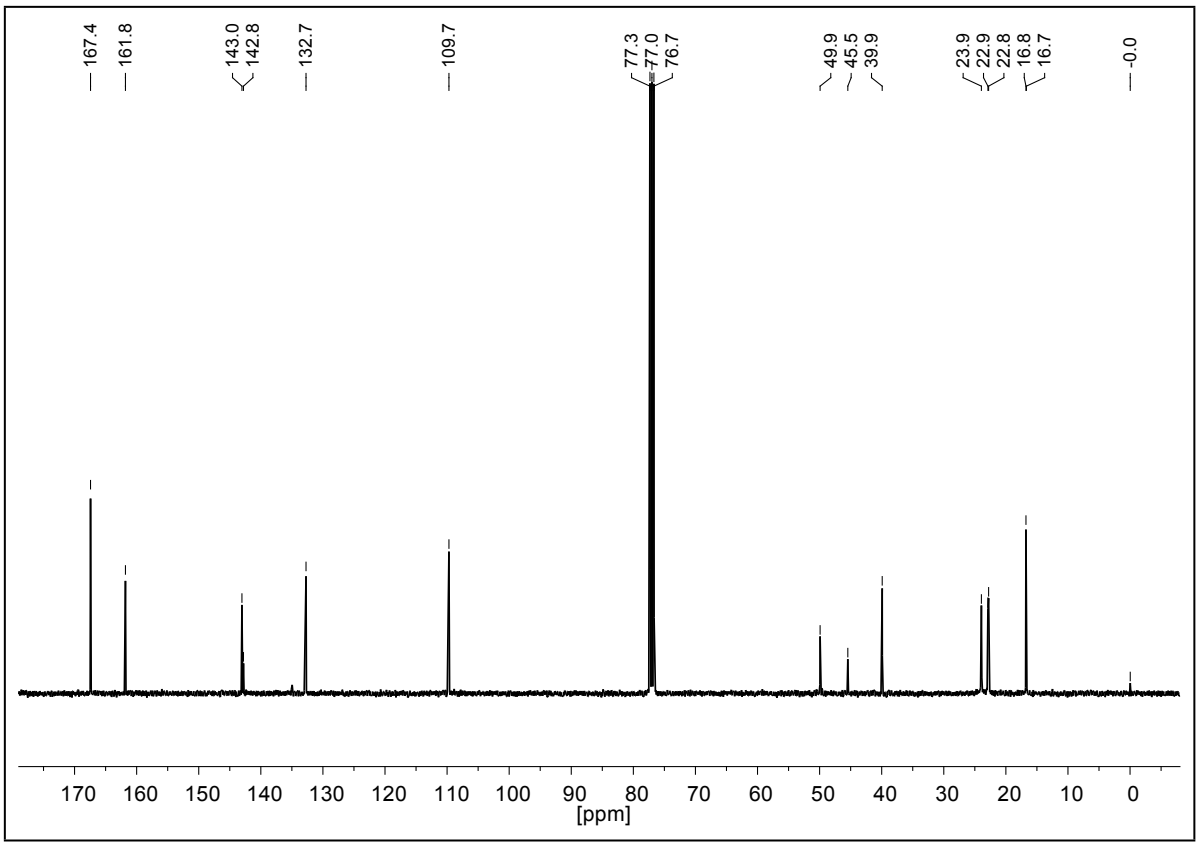

Figure S23. ^{13}C NMR spectrum of **10** in $CDCl_3$.

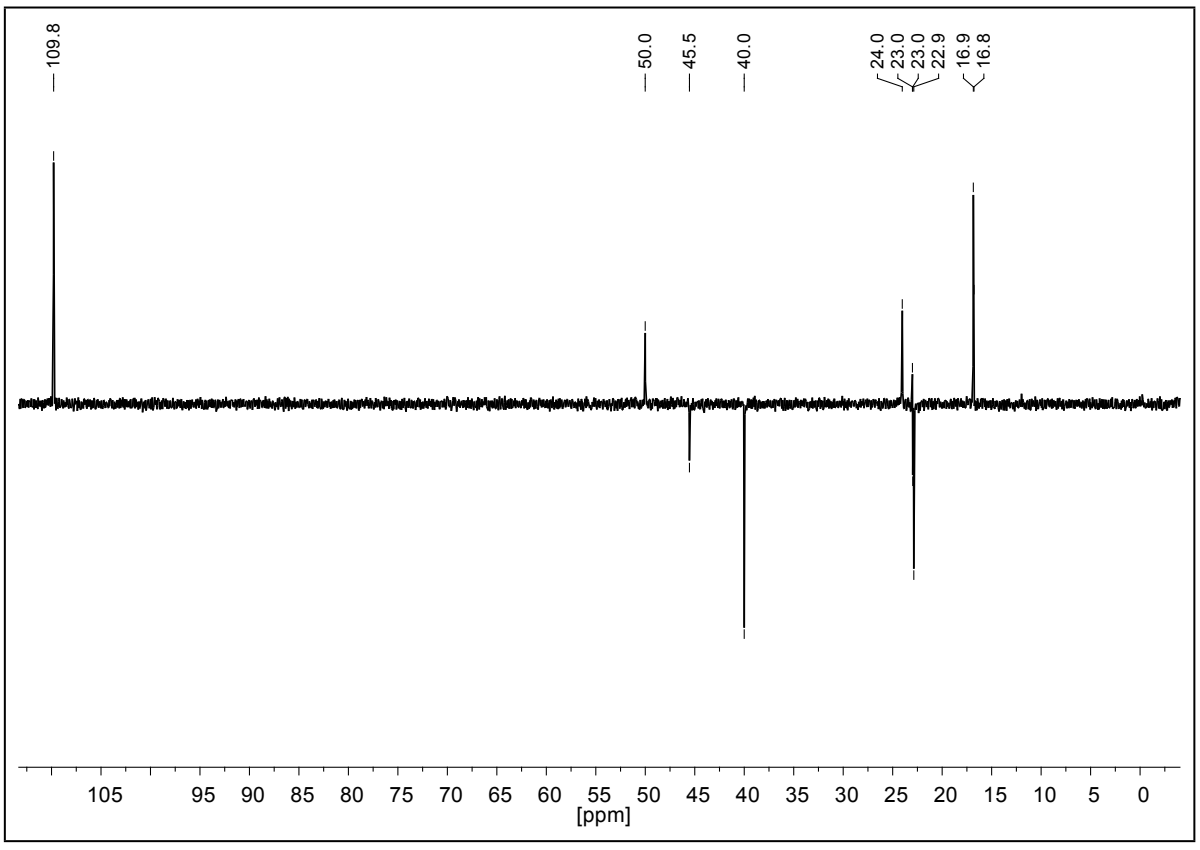

Figure S24. DEPT spectrum of **10** in $CDCl_3$.

7.4 ^{1}H and ^{13}C NMR spectra of compound **12**.

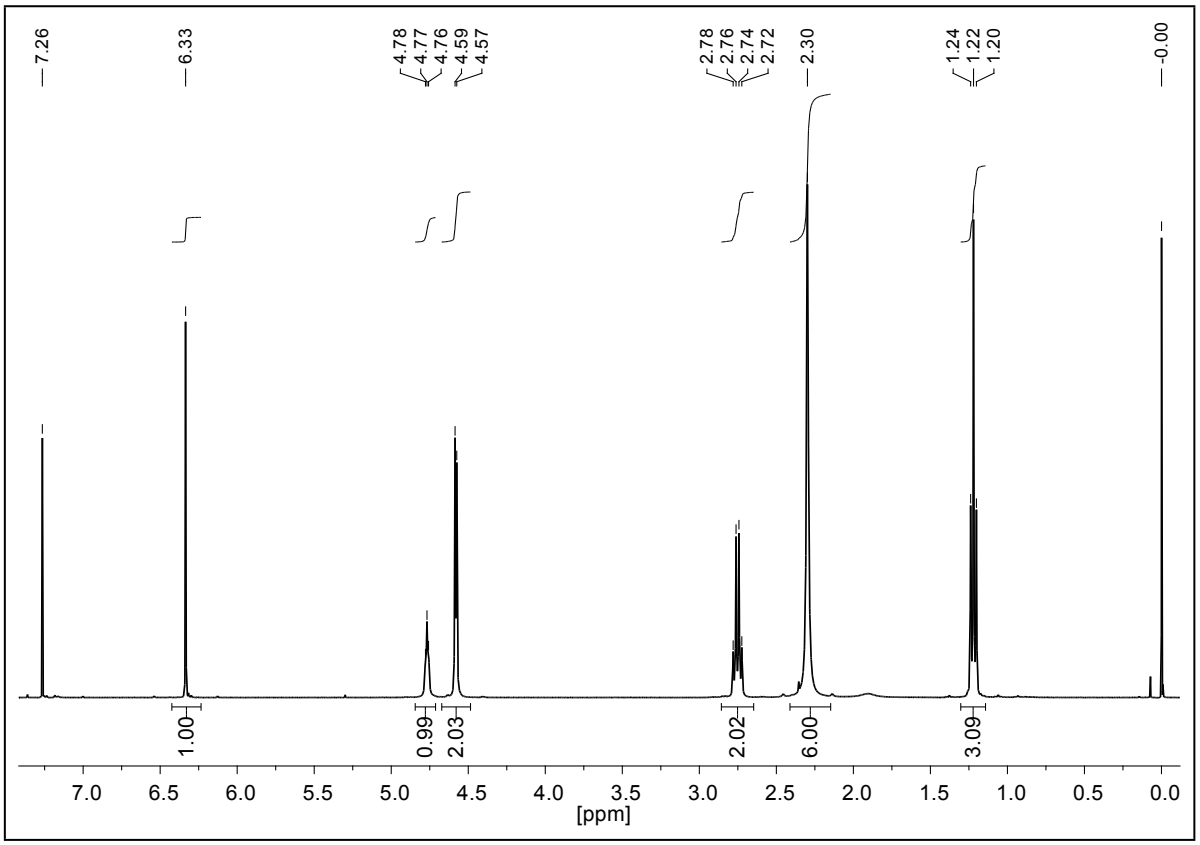

Figure S25. ^{1}H NMR spectrum of **12** in $CDCl_3$ (0.06 M).

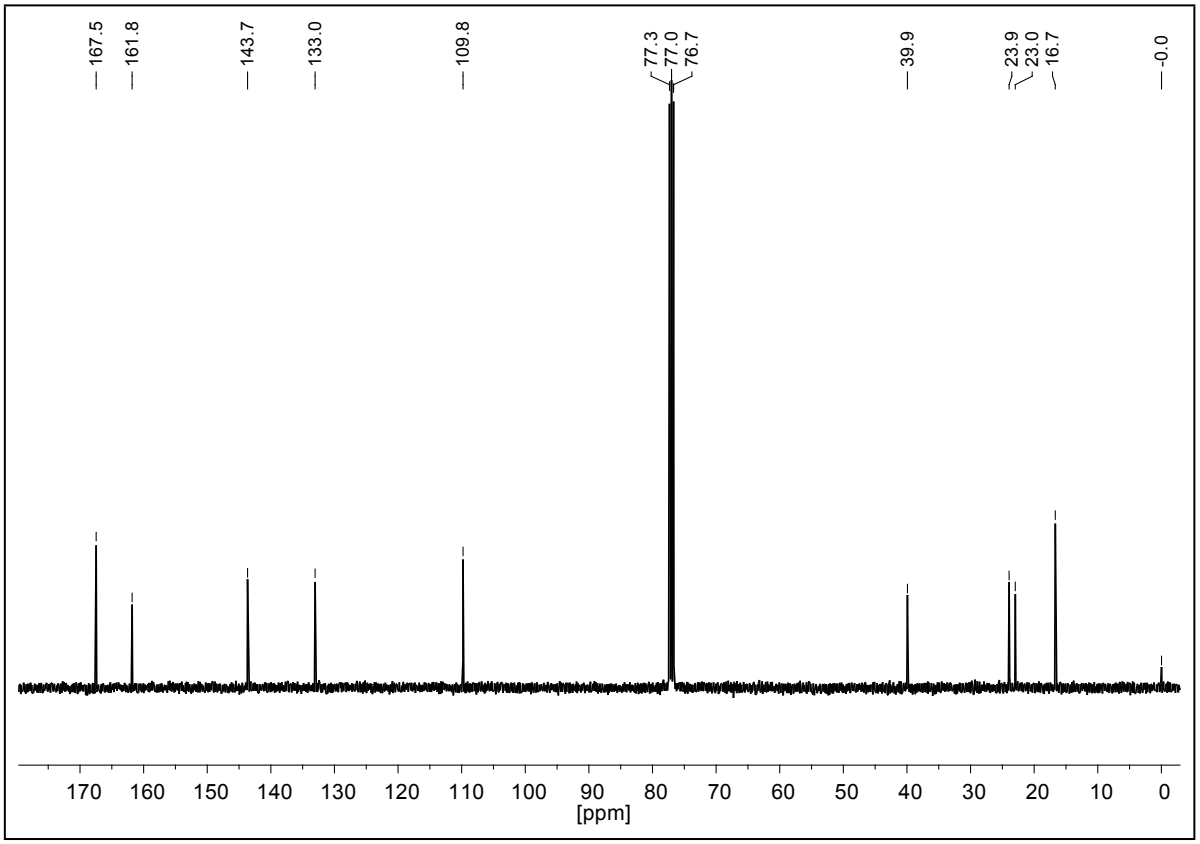

Figure S26. ^{13}C NMR spectrum of **12** in $CDCl_3$.

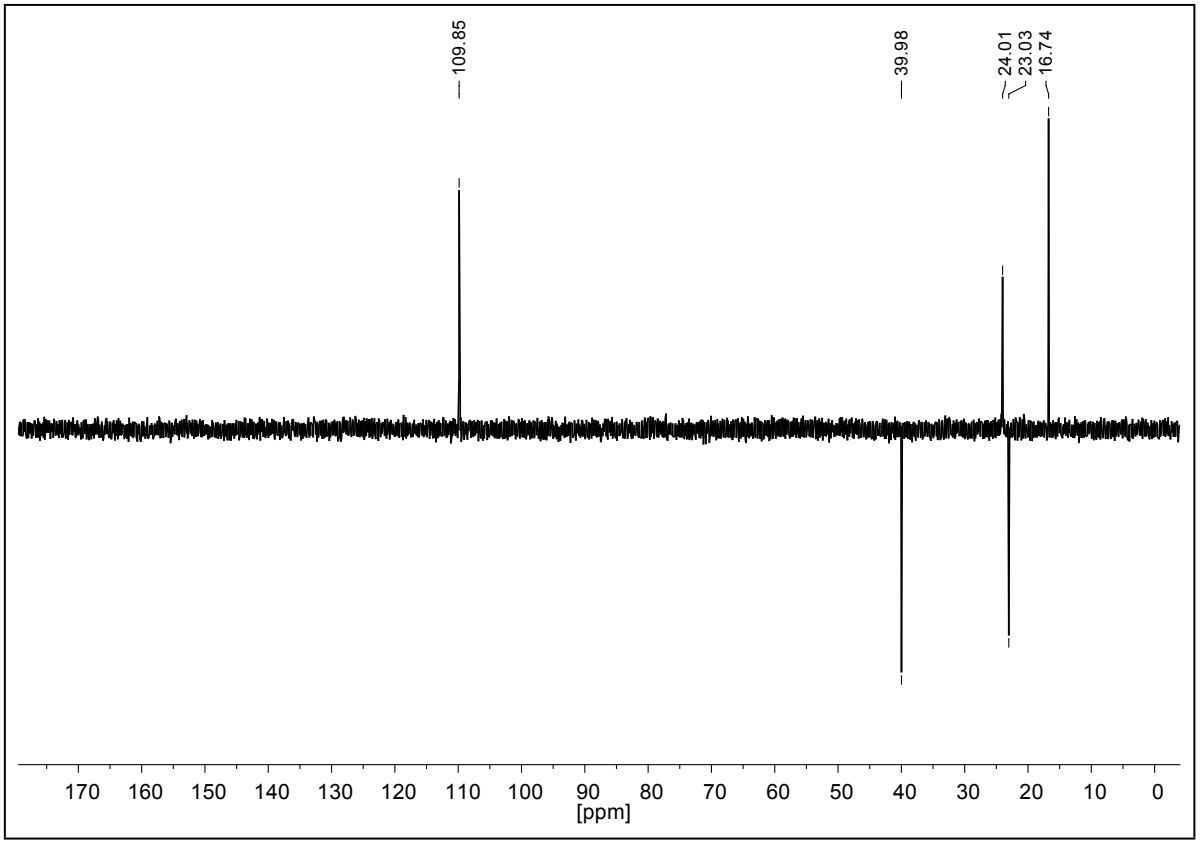

Figure S27. DEPT spectrum of **12** in $CDCl_3$.

7.5 ^{1}H and ^{13}C NMR spectra of compound **13**.

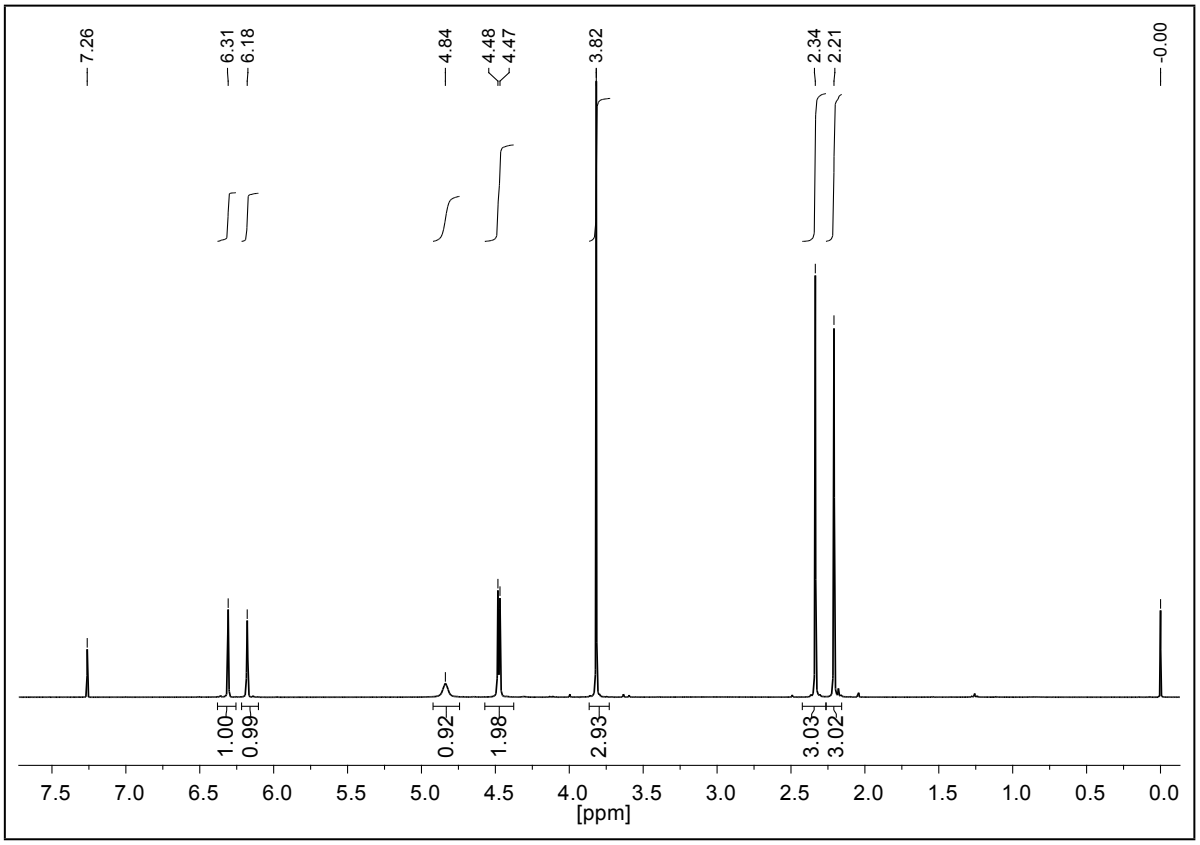

Figure S28. ^{1}H NMR spectrum of **13** in $CDCl_3$ (0.03 M).

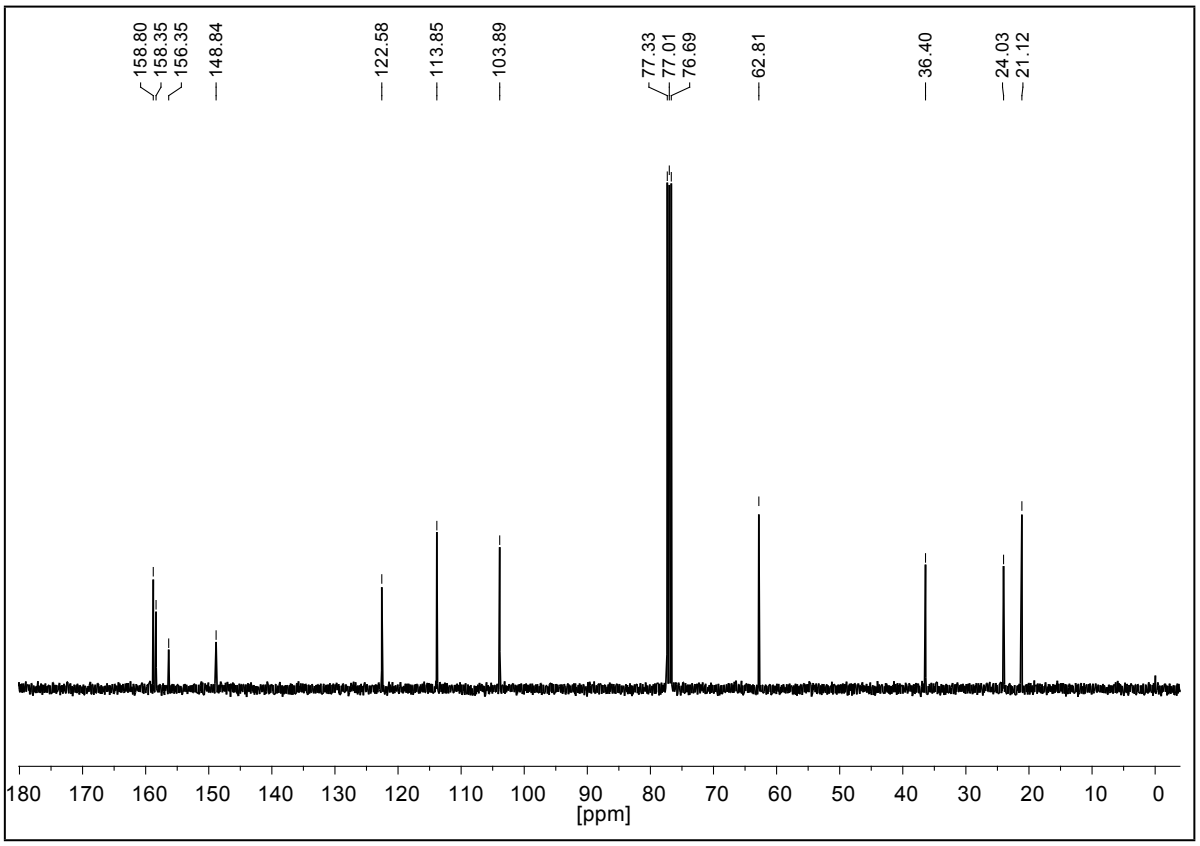

Figure S29. ^{13}C NMR spectrum of **13** in $CDCl_3$.

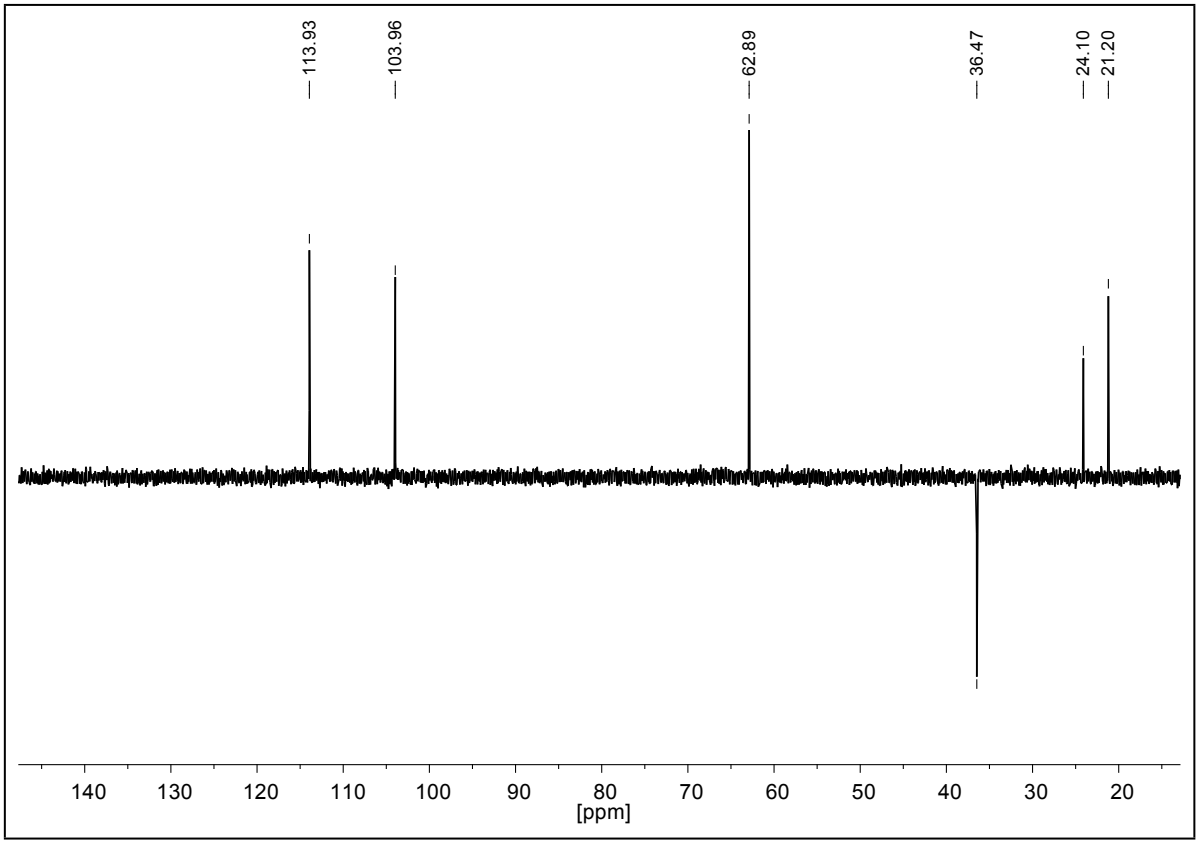

Figure S30. DEPT spectrum of **13** in $CDCl_3$.

7.6 ^{1}H and ^{13}C NMR spectra of compound **14.**

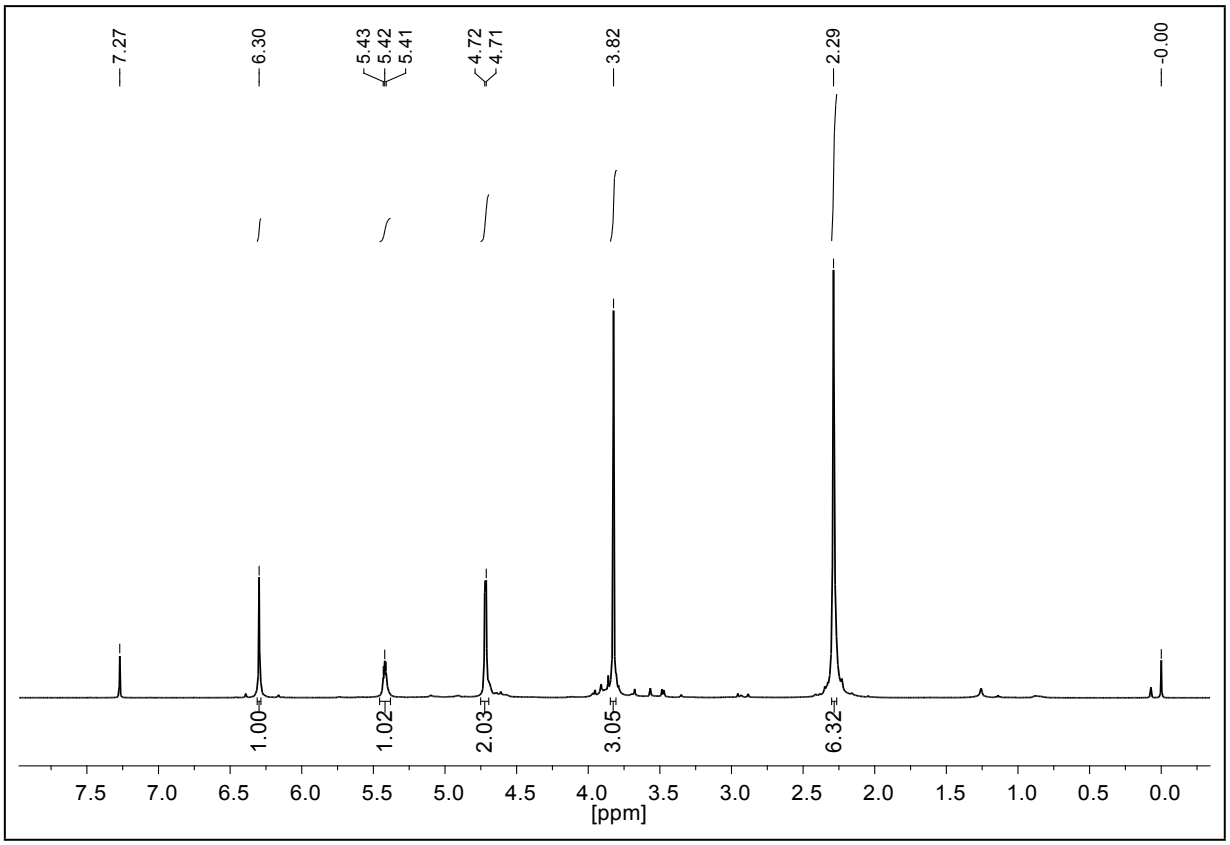

Figure S31. ^{1}H NMR spectrum of **14** in $CDCl_3$ (0.02 M).

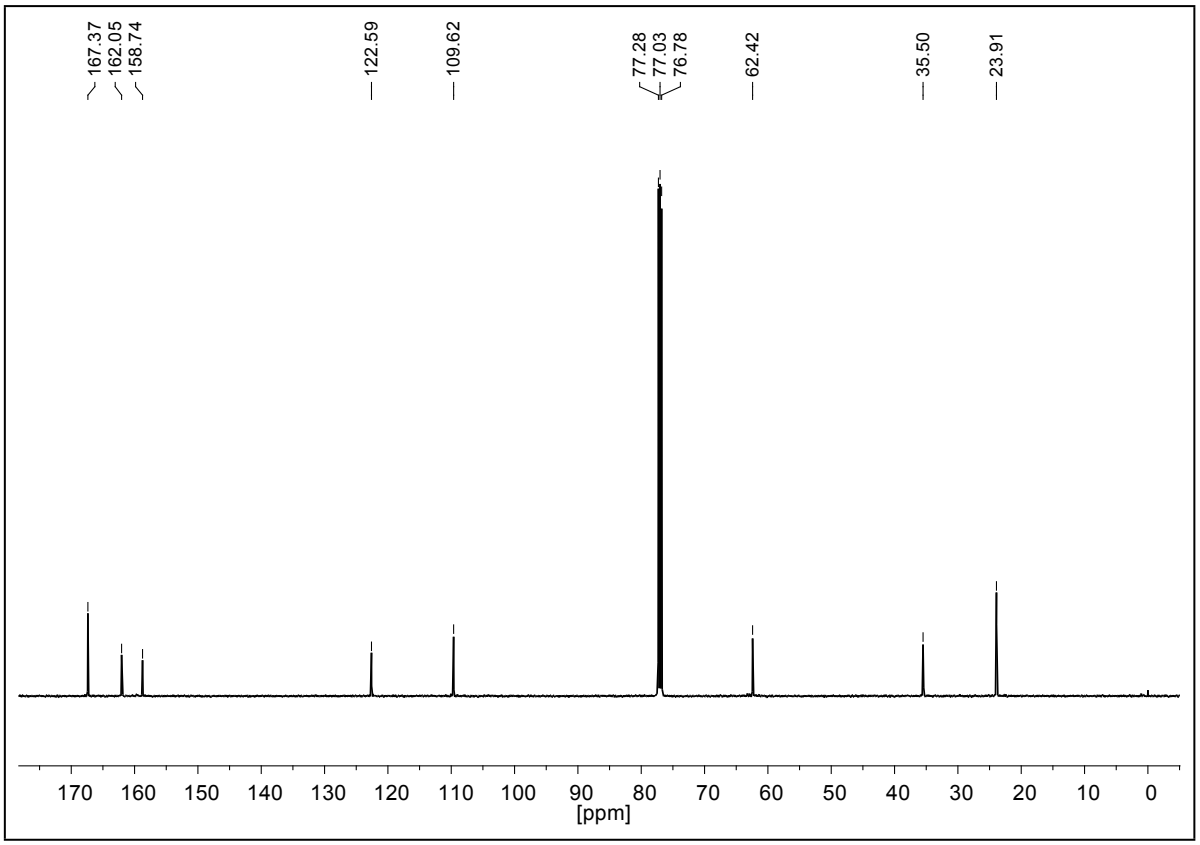

Figure S32. ^{13}C NMR spectrum of **14** in $CDCl_3$.